Colloid Polym Sci 274:191–196 (1996)

ORIGINAL CONTRIBUTION

C. Fülber
K. Unseld
V. Herrmann
K.H. Jakob
B. Blümich

In situ investigation of SBR vulcanization: A combined study of ^{1}H-NMR and vulcametry

Received: 29 May 1995
Accepted: 18 August 1995

C. Fülber · Prof. Dr. B. Blümich (✉)
Makromolekulare Chemie
RWTH Aachen
Worringerweg 1
52056 Aachen, FRG

K. Unseld · V. Herrmann · K.H. Jakob
Dunlop SP Reifenwerke GmbH
Dunlopstraße 2
63450 Hanau, FRG

C. Fülber
Max-Planck-Institut für Polymerforschung
Ackermannweg 10
55021 Mainz, FRG

Abstract For the first time, in situ NMR measurements were performed during sulfur vulcanization of unfilled SBR. A vulcanization device was constructed for use in combination with a standard microimaging probe in a vertical bore NMR magnet. ^{1}H-linewidth measurements are correlated with cure simulations in a vulcameter to explain the increase of the linewidth during the vulcanization. Inhomogeneous heating conditions in the sample result in an inhomogeneous course of the vulcanization as a function of time. The spatial dependence of this process was monitored by NMR imaging.

Key words Vulcanization – NMR – NMR imaging – vulcametry – cure simulations

Introduction

Crosslinked elastomers at temperatures above T_g are rewarding materials for the application of ^{1}H-NMR methods such as spectroscopy [1] and imaging [2]. This is due to their richness in protons and their small static ^{1}H-linewidth of < 2.5 kHz at room temperature. In spite of the suitability of NMR, such measurements were never performed in situ during the vulcanization process. The curing of phenolic and epoxy resins, a process formally related to vulcanization, has only recently been investigated by NMR methods [3, 4].

Since its discovery by Goodyear (1839), the vulcanization process is of outstanding importance for the manufacturing of high yield elastomers and rubbers. The standard method for monitoring the crosslinking process is vulcametry [5]. The goal of this paper is to investigate the use of standard ^{1}H-NMR methods for the analysis of the vulcanization process in elastomers and correlate the results to vulcametric measurements. The investigated elastomer material was an SBR or poly(styrene-co-butadiene) system.

For the NMR measurements, an apparatus was constructed for in situ vulcanization under realistic conditions inside the NMR magnet. The requirements were twofold: First, sufficient pressure was needed to ensure homogeneous vulcanization, and second, sufficient heating was necessary in order to observe the reaction on an acceptable timescale.

It is demonstrated that the crosslinking process can be followed by ^{1}H-linewidth measurements. These data are correlated to vulcameter measurements of the shear modulus. This assumes that the transverse ^{1}H magnetization decay can be described by an exponential function with a single time constant. This is a justified approximation for the measurements reported here, which were carried out in slightly inhomogeneous magnetic fields. In

Colloid & Polymer Science, Vol. 274, No. 3 (1996)

homogeneous magnetic fields, it is known that the transverse ^1H magnetization decay is nonexponential in crosslinked elastomers and depends on the crosslink density [6–9].

In a second step, an NMR imaging experiment is reported by which inhomogeneities in space and time of the vulcanization process can be followed. These inhomogeneities are caused by the heating geometry and the heat transport properties of the sample.

Experimental

The NMR measurements were performed on a Bruker MSL Spectrometer at a ^1H frequency of 300 MHz. A vulcanization device (VD) was constructed to fit into a commercial Bruker micro-imaging probe. The design is depicted in Fig. 1. The VD was inserted form the top into a 79 mm vertical bore magnet to fit into an Alderman–Grant saddle coil [10]. This coil had an inner diameter of 23 mm. The vertical position within the coil was adjusted by a Teflon spacer so that the sample chamber was in the sensitive region of the B_1-coil.

Cooling with air was necessary to protect both the probe and the inner bore of the magnet from overheating. A steel spring (D = 11.5 N/mm) was employed to provide a minimum pressure of 400 kPa (4 bar) during vulcanization. The particular pressure on the spring was controlled by an adjustable nut. The heating cartridge was equipped with a thermocouple (NiCr/Ni) which allowed the observation of the cartridge temperature. A simple manual control of the heating current was found to be sufficient for the experiment. An NMR measurement with a thermo-couple inserted in the sample chamber is not feasible because the metallic wire becomes an antenna for stray signals during data acquisition. In order to determine the average temperature of the sample as a function of time, each experiment was repeated without NMR data acquisition under the same heating conditions defined by the cartridge current. Knowledge of this temperature curve is necessary for comparison of the NMR results with the cure simulation in the vulcameter. For the experiments shown below the curves always showed an increase of temperature in the first 10 min and a constant value afterwards. Hence the conditions were isothermal after 10 min.

The operation of the VD with samples of 100 mg to 200 mg was found to be optimum with respect to a compromise which had to be found between heating conditions and NMR measurements: Although larger samples would provide a better filling factor for the NMR coil and hence a better signal-to-noise ratio, homogeneous vulcanization could no longer be assured. In fact, inhomogeneous vulcanization could be followed by NMR imaging (see below).

The cure simulations were performed on a Monsanto vulcameter MDR-2000-E [11] which allowed programming of the temperature curves used in the NMR experiments. The vulcanization system of the investigated sample is shown in Table 1. A standard accelerator of the TBBS-type has been used.

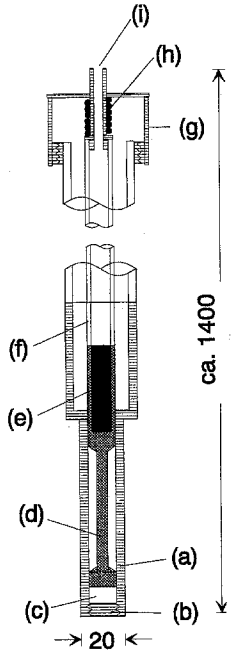

Fig. 1 Vulcanization device: (a) Polyimide case, (b) polyimide muzzle with screw top, (c) sample chamber, (d) copper piston, (e) heating cartridge, (f) ceramic connecting rod, (g) brass nut with thread for pressure control, (h) steel spring, (i) access for ventilation and wiring. All measures are given in mm

Results and discussion

NMR relaxation measurements

Only one-pulse free-induction decay signals (FIDs) were recorded in the first experimental stage. The reasons were twofold: 1) Ferromagnetic parts in the VD caused B_0-field inhomogeneities which gave rise to fast signal decays and prevented accurate settings of pulse times. 2) The

Table 1 Vulcanization system

Material	Amount [phr]
SBR Buna® 1500	100
ZnO	3
Stearic acid	2
S	3
Accelerator	3

timescale of the vulcanization process in the chosen temperature region is in the order of minutes. To monitor such fast processes, a simple acquisition scheme was needed.

The FIDs were recorded on resonance and the signal in the time domain was subsequently fitted to a single exponential. The characteristic decay time constant is denoted by T_2^* with $R_2^* = 1/T_2^*$ the decay rate which is proportional to the linewidth.

A typical curve of T_2^* as a function of time is displayed in Fig. 2. The curve is characterized by three distinct regions: The first region is defined by a rise of T_2^* up to a maximum value during the first 10 min due to the temperature increase in the sample. In the second region T_2^* decreases at constant temperature. This is attributed to the vulcanization. The third region is identified by a plateau with a constant value of T_2^* after the end of the reaction. After the experiment, a flat vulcanized rubber cylinder is removed from the sample chamber.

The validity of this interpretation of the data in Fig. 2 was checked by using a compound which contained only the polymer and no other additives. Hence vulcanization could not take place. In fact, the increase of T_2^* at the beginning of the curve was observed as well as the plateau region in the end at constant sample temperature, but the characteristic decrease of the curve in the second region of Fig. 2 was absent. This proves that vulcanization indeed causes this feature in Fig. 2. Vulcanization can indirectly be mapped by following T_2^* with the given experiment.

The region of interest for further analysis is the decrease in T_2^* due to vulcanization. This decay corresponds to an increase in the shear modulus G' in the vulcameter, which is elaborated in the following. For reasons of simplicity the shear modulus is reduced to a relative value x_r:

$$x_r = \frac{G' - G_{min}}{G_{max} - G_{min}} . \quad (1)$$

For adequate comparison of NMR and vulcametric measurements, it is essential that the temperature curve $T = T(t)$ of the sample is known and can be used for measurement of the shear modulus in the vulcameter. The temperature curve $T(t)$ was acquired as described above. Having measured the shear modulus as a function of time $x_r = x_r(t)$ in the vulcameter with the temperature curve of the NMR experiment, it can be correlated to the NMR relaxation rate $R_2^* = R_2^*(t)$ to eliminate the time dependence:

$$R_2^*(t),\ x_r(t) \xrightarrow[T(t)]{} R_2^*(x_r) . \quad (2)$$

As $R_2^*(t)$ and $x_r(t)$ are both measured at discreet points in time, which in general are not identical, one of the functions had to be parameterized for interpolation to arbitrary times t. T_2^* was chosen, because the parameterization can also serve to smooth the NMR data. $R_2^*(t)$ was calculated afterwards from the parameterized curve of T_2^*.

The function $F(t, a, b, c \ldots)$ for parameterization was chosen to fit the shape of $T_2^*(t)$ in the regions II and III of Fig. 2. In particular, it had to reproduce the maximum in T_2^* at the onset of vulcanization at time t_i as well as the plateau at the end of the reaction (Fig. 2). Figure 3 shows the region of interest with two different polynomials fitted to the experimental data. The solid line is for a polynomial of degree 3 and the broken line for a polynomial of degree 4. The corresponding values of the reduced modulus x_r and the mechanical loss factor $\tan\delta$ as a function of time t are shown in Fig. 4. Combining the NMR and vulcametric data according to Eq. (2) leads to the correlation of NMR relaxation rate and mechanical modulus shown in Fig. 5. For the experiment leading to Figs. 2, 3 and Fig. 5, 180 mg of sample were prepared. From the heating curve an initial time $t_i = 30.4$ min between the beginning of heating and the onset of vulcanization was observed. The final sample temperature under isothermal conditions was 142 °C. The correlation in Fig. 5 covers the range from $t = 31$ min to $t = 44$ min. The two sets of data points correspond to fits of third and fourth order polynomials for the T_2^* curves (cf. Fig. 3).

A second example for a correlation under different experimental conditions is shown in Fig. 6. Only 110 mg of sample were vulcanized here. A higher sample temperature during vulcanization (152 °C) was chosen than for the measurement of Fig. 5 resulting in $t_i = 17.5$ min. Both figures show an increase in the linewidth which is approximately linear except for extreme values of the reduced shear modulus. The characteristic S-shape of the curve may be an artifact.

Fig. 2 Typical T_2^*-curve corresponding to the measurement in Fig. 5. Three distinct regions are discriminated: I) Increase in T_2^* due to the heating-up process of the sample chamber. II) Decrease in T_2^* during vulcanization. III) Plateau region following the completion of the reaction

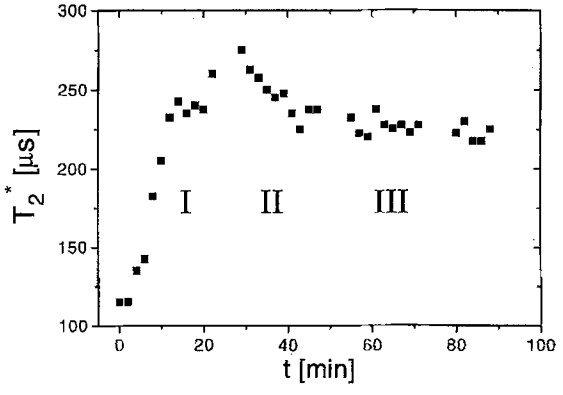

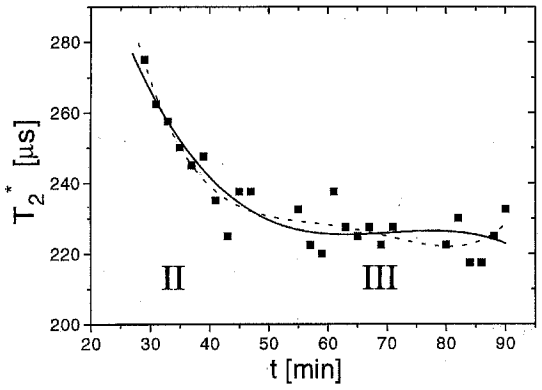

Fig. 3 Regions II and III of Fig. 2 with two fits. Solid line: Polynomial of degree 3. Broken line: Polynomial of degree 4

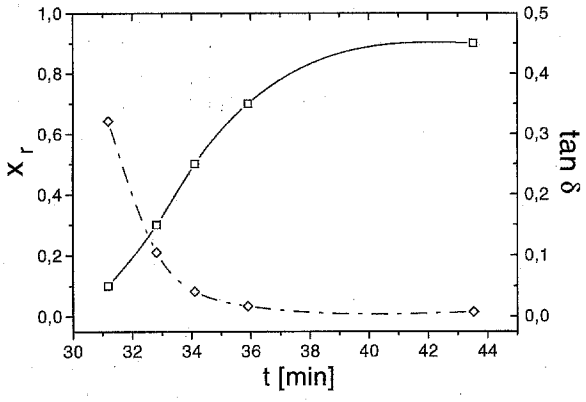

Fig. 4 Vulcameter-curve: Measurement of the torque in a low frequency shear experiment (1 Hz) as a function of time. This curves corresponds to the experimental conditions in Figs. 2, 3 and 5. Additionally, the loss factor $\tan\delta$ is plotted (broken line)

With the equipment used in the experiment described above, the relaxation rate was measured in an inhomogeneous field because of slightly ferro-magnetic heater material. The experimentally determined relaxation rate can be decomposed into two parts,

$$R_2^* = \frac{1}{T_2^*} = \frac{1}{T_2} + \frac{1}{T_2^{B_0}}, \tag{3}$$

where $1/T_2^{B_0}$ describes the contribution of the static field inhomogeneity and $1/T_2$ is the transverse relaxation rate determined by the material properties and affected by the vulcanization process. Due to the field inhomogeneity, the ratio of contributions to the linewidth which are affected and those which are unaffected by the vulcanization is only about 1/9. Nevertheless, the correlation achieved in Figs. 5 and 6 is substantial, because the $1/T_2^{B_0}$ term results in a constant offset of about 4 kHz which can be subtracted.

$1/T_2$, on the other hand, is given by the theory of Bloembergen, Purcell and Pound [12], which is in our case

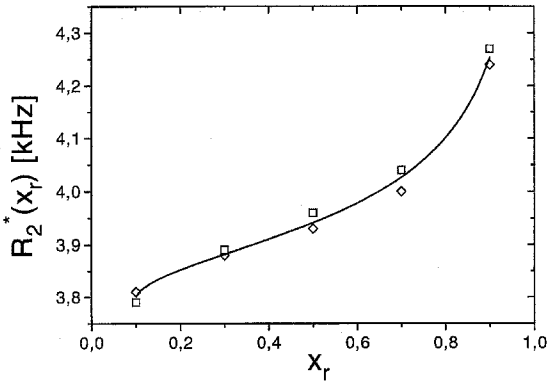

Fig. 5 First experimental correlation of R_2^* with x_r for the experimental conditions of Fig. 2: 180 mg sample, $t_i = 30.4$ min, vulcanization temperature 142 °C. The correlation covers the range from $t = 31$ min to $t = 44$ min. Diamonds: Fit of T_2^* data with a polynomial of degree 3. Squares: Fit of T_2^* data with polynomial of degree 4. The solid line is drawn to guide the eye

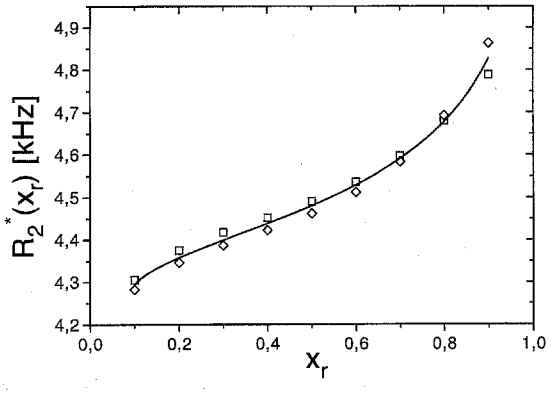

Fig. 6 Second experimental correlation of R_2^* with x_r. Experimental conditions: 110 mg sample, $t_i = 17.5$ min, 152 °C sample temperature. Diamonds: Fit of T_2^* data with polynomial of degree 3. Squares: Fit of T_2^* data with a polynomial of degree 4. The correlation covers the range from $t = 18$ min to $t = 25$ min. The solid line is drawn to guide the eye

valid for rubbers at about 150 °C:

$$\frac{1}{T_2} = \sum_{i=1}^{3} J_i \frac{\tau}{1 + \omega_i^2 \tau^2}. \tag{4}$$

Here, J_i denote the amplitudes of the spectral densities and $\omega_i = 0$, ω_0, and $2\omega_0$, where $\omega_0 = 300$ MHz is the Lamor-frequency of the spectrometer used. In the limit of $\omega_0\tau \gg 1$, i.e., for the slow molecular motion, all terms except the first one are negligible:

$$\frac{1}{T_2} = J_1 \tau. \tag{5}$$

This gives a dependence of the linewidth on one single correlation time. This correlation time must be affected by

the increase in the crosslinking during the vulcanization process. And hence it is the link between vulcametry and NMR.

This assumption is a simplification in two respects:

1) The molecular motion is in general a distribution of correlation times extending over many decades [13].

2) The equivalence between the correlation times of molecular motion relevant to NMR and those relevant to mechanical measurements is not evident a priori. Nevertheless, such an approach has been used in the work of Marcinko and Parker [14–16] who have postulated a correlation of the cross-polarization rate $1/T_{CH}$ and the dynamic modulus for a variety of polymers on the basis of the Maxwell model. Given the objections above, a more than qualitative analysis of the correlation between NMR and mechanical properties cannot be formulated at this time.

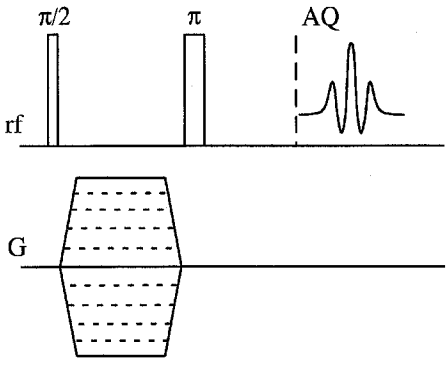

Fig. 7 Basic pulse sequence for phase-encoded spatial resolution. The magnetic field gradient G is incremented step by step in successive experiments. Fourier-transformation of the echo amplitude as a function of the gradient strength introduces the spatial resolution. 'rf' denotes radio frequency excitation with pulse flip angles given by $\pi/2$ and π. AQ indicates data acquisition

NMR imaging results

In the vulcanization device, heat is administered to the sample by a copper piston from one side only. For samples of thickness $\Delta d > 1$ mm the heating conditions can be assumed to be inhomogeneous. Careful positioning of the thermocouple indicated a temperature range of 140 °–170 °C across a length of $\Delta d = 2$ mm of the sample. By NMR imaging the resulting inhomogeneities of the vulcanization process can be followed in space and in time.

Because of the presence of large B_0-field inhomogeneities, the standard spin-echo imaging [10] sequence could not be employed. A remedy was found in using a single phase-encoding gradient to obtain spatial resolution (Fig. 7), because the phase encoded dimension is not affected by B_0-field inhomogeneities.

By this technique, one-dimensional spatial projections were recorded with the z-direction along the cylinder axis of the sample as the spatial dimension using 16 increments of the phase-encoding gradient. The image contrast is based on T_2^* weighting of the acquired signal. Thus, the contrast indicates differences in T_2^* which scale with differences in the increasing crosslink density. The acquisition of one projection required eight acquisition cycles with a recycle delay of 1.4 s. Hence each projection reflects the conditions within the sample averaged over 3 min.

In Fig. 8, the measured projections are depicted for different times elapsed since the start of the vulcanization experiment. After 5 min the image contrast only reflects the temperature gradient over the sample from right to left. The projection after 15 min shows a sharp decrease in the contrast parameter on the right-hand side: The vulcanization is already completed there, whereas on the left-hand side the reaction has only started. After 35 min, the reaction is finished across the whole sample. Only on the left-hand side an increase in the contrast parameter remains, probably caused by the influence of the cooled bottom of the vulcanization device.

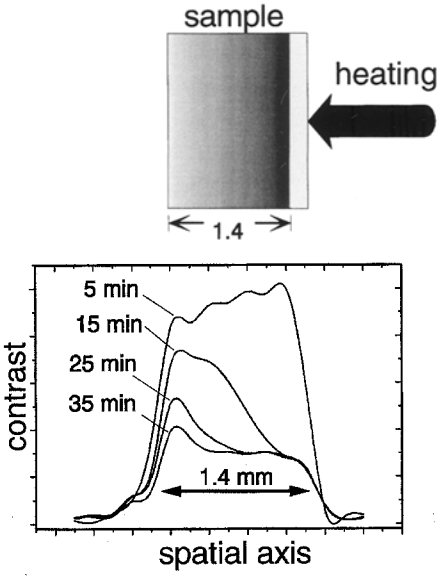

Fig. 8 Phase-encoded projections along the z-dimension of the elastomer sample. For encoding of the spatial dimension 16 gradient increments were employed. The inhomogeneous vulcanization process becomes evident

In Fig. 9, the course of the contrast parameter in the images of Fig. 8 is shown as a function of time for four different points in space. The individual curves are spaced about 0.5 mm apart. The onset of the vulcanization is marked in the picture for the different points in space which manifests itself as a change in the curvature of the contrast parameter curves.

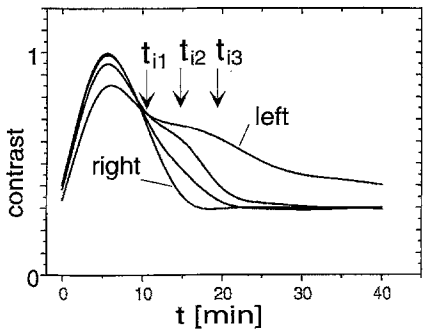

Fig. 9 The contrast parameter of the phase-encoded projections as a function of time (cf. Fig. 8). Along the time axis 11 projections were recorded and connected by spline interpolation. The onset of the vulcanization process is marked by t_i for three points in time

From the viewpoint of NMR this experiment is an example for a case in which phase-encoded imaging is obligatory due to the large B_0-field inhomogeneity. From the perspective of vulcametry, this measurement delivers information about the spatial and time dependence of the type of inhomogeneous vulcanization conditions encountered in practice.

Summary

The reported work intends to extend the possibilities of NMR for the routine industrial application in the field of elastomers. The process of vulcanization is well understood from the viewpoint of viscoelastic and rheological measurements. It has not been investigated by in situ NMR before. For in situ measurements an apparatus was constructed which would both provide the necessary conditions for vulcanization and fulfill the limitations of an established NMR environment. Linewidth measurements were performed during the vulcanization because they are rapid enough for the timescale of the reaction. The detrimental effect of an inhomogeneous B_0 field is understood and can be subtracted. It has been shown that the established vulcametric measurements correlate well with NMR measurements giving an increase in the linewidth with an increasing degree of vulcanization. The central assumption for interpretation of this observation is that the correlation time for the molecular motion manifests itself in both the dynamic behavior of the modulus and in the NMR relaxation.

Inhomogeneous vulcanization conditions were visualized by NMR imaging. The drawback of B_0-field inhomogeneities was overcome by phase-encoding of the spatial axis. Different time dependencies of the vulcanization process were identified for sample regions with different separations from the heat source.

Acknowledgments The work has been supported in part by the Deutsche Kautschukgesellschaft. We thank Prof. Spiess for the possibility to conduct the NMR measurements in the Max-Planck-Institut für Polymerforschung, Mainz, and helpful discussions.

References

1. Komoroski RA (ed) (1986) High Resolution NMR Spectroscopy of Synthetic Polymers in Bulk, VCH Publishers, Deerfield Beach FL
2. Blümich B, Kuhn W (eds) (1992) Magnetic Resonance Microscopy: Methods and Applications in Materials Science, Agriculture and Biomedicine, VCH Publishers, Weinheim
3. Neiss TG, Vanderheiden EJ (1994) Macromol Symp 86:117–129
4. Barton JM, Buist GJ, Hamerton I, Brendan JH, Jones JR, Liu S (1994) Polymer Bulletin 33:215–219
5. Schnetger J (1991) Lexikon der Kautschuktechnik, Hüthig und Wepf Verlag, Heidelberg
6. Fedotov VD, Schneider H (1989) Structure and Dynamics of Bulk Polymers by NMR-Methods In: Diehl P (ed) NMR Basic Principles and Progress 21. Springer Verlag, Heidelberg
7. Cohen-Addad JP, Dupeyre R (1993) Polymer 24:400–408
8. Brereton MG (1990) Macromolecules 23:1119–1131
9. Kulagina TP, Litvinov VM, Summanen KT (1993) J Polym Sci, Part B Polym Phys 31:241–248
10. Callaghan PT (1991) Principles of Nuclear Magnetic Resonance Microscopy, Clarendon Press, Oxford
11. Burhin HG (1992) Kautschuk und Gummi, Kunststoffe 45:866–870
12. Abragam A (1961) Principles of Nuclear Magnetism, Clarendon Press, Oxford
13. Schmidt-Rohr K, Spiess HW (1994) Multidimensional Solid-State NMR and Polymers, Academic Press, London
14. Parker AA, Marcinko JJ, Rinaldi P, Hedrick DP, Ritchey WM (1993) J Appl Polym Sci 48:677–681
15. Marcinko JJ, Parker AA (1994) Macromol Symp 86:251–257
16. Marcinko JJ, Parker AA, Rinaldi PL, Ritchey WM (1993) Polym Mater Sci Eng 68:266–267